

FITTING HYPERBOLIC UNIVERSES TO CAYÓN-SMOOT SPOTS IN COBE MAPS

HELIO V. FAGUNDES

Instituto de Física Teórica, Universidade Estadual Paulista, Rua Pamplona, 145, 01405-900 São Paulo, SP, Brazil; helio@ift.unesp.br

Received 1995 November 2; accepted 1996 April 22

ABSTRACT

On the possibility that the universe's matter density is low ($\Omega_0 < 1$), cosmologies can be considered with the metric of Friedmann's open universe but with closed hyperbolic manifolds as the physical three-space. These models have nontrivial spatial topology, with the property of producing multiple images of cosmic sources. Here a fit is attempted of 10 of these models to the physical cold and hot spots found by Cayón & Smoot in the COBE/DMR maps. These spots are interpreted as early, distant images of much nearer sources of inhomogeneity. The source for one of the cold spots is seen as the seed of a known supercluster.

Subject headings: cosmic microwave background — cosmology: theory

1. INTRODUCTION

The maps of cosmic microwave background (CMB) produced from data of the Differential Microwave Radiometer (DMR) on the *Cosmic Background Explorer* (COBE) satellite (Smoot et al. 1992; Bennett et al. 1994) are usually analyzed in terms of their spherical harmonics decomposition of the temperature fluctuations (Wright et al. 1994; White, Scott, & Silk 1994, and references therein). But a few studies have focused on individual “cold” and “hot” spots in those maps, trying to separate the physical ones (overdense and underdense regions) from those produced by instrumental noise. Thus Torres (1994) has analyzed the spots from the first-year COBE/DMR anisotropy maps and found a number of candidates for physical spots. The author (Fagundes 1995) has given an interpretation of overdense spots in terms of images of primordial seeds in compact, topologically nontrivial universes, which is also the basis of the present work (see below). Cayón & Smoot (1995, hereafter CS), using a method similar to that of Torres (1994), studied the data of the first 2 years of the COBE/DMR experiment to find spots that appear simultaneously in three frequencies (31, 53, and 90 GHz); their significance is determined through comparison with Monte Carlo noise simulations. Figure 1 is a Mollweide map of the CS spots.

In this paper, I use the six cold and eight hot spots obtained by CS for the case of no restriction on the number of common pixels per spot in the three channels. They estimate as less than 12.5% the chance that these spots are produced by noise.

Closed hyperbolic universe models have been considered by the author on a number of occasions: see Fagundes (1993), and references therein. These models have the space-time metric of Friedmann's open model; see Landau & Lifshitz (1975), § 113, p. 366:

$$ds^2 = c^2 dt^2 - a^2(t) d\lambda^2 \quad (1)$$

where

$$d\lambda^2 = d\chi^2 + \sinh^2 \chi (d\theta^2 + \sin^2 \theta d\phi^2), \quad (2)$$

is the metric of comoving space. But while the time coordinate varies from 0 to infinity (as in the open model), comoving space is taken to be a *closed hyperbolic manifold* (CHM), that is, a closed space with the metric given in equation (2) and hence of negative curvature ($K = -1$). A

CHM, and hence a closed hyperbolic universe, has a nontrivial global topology (see Lachièze-Rey & Luminet 1995, and references therein), which leads to the outstanding property of the production of multiple images of cosmic sources; see § 2.

The idea of this work is to consider 10 such universes, with the 10 smallest known orientable CHMs (Hodgson & Weeks 1994) as the comoving three-space. In § 3 they are adjusted so that the CS spots appear as distant, topologically produced images of nearby seeds. One of the seeds for overdense (“cold”) spots is interpreted tentatively as the precursor of a known supercluster. Final comments are made in § 4.

2. CLOSED HYPERBOLIC UNIVERSES

As stated above, closed hyperbolic universes have closed hyperbolic manifolds (or spaces) as the comoving space. A CHM can be obtained by identification of pairs of faces of a Dirichlet domain, or *fundamental polyhedron* (FP) in hyperbolic space H^3 ; the latter is then tessellated (i.e., divided) into a “honeycomb” of cells that are replicas of the FP. These replicas are obtained by the action of a discrete group Γ of rigid motions of H^3 ; see, for example, Ellis & Schreiber (1986) and Fagundes (1989).

Real space is then the CHM, so it can be represented by the FP with identified (or “glued together”) pairs of faces. Due to the nontrivial topology, a source's ray starting in the FP can reach the observer (also in the FP) through different paths, and so it may produce images apparently coming straight from other cells. Since the FP can be chosen smaller than the radius of the observed universe, the idea is that only a fraction of the images of cosmic objects we detect come directly from the sources, the other being indirect, or topological, images of those sources. Some authors call the latter “ghosts.” But physically there is no difference between direct or indirect images; besides, this classification depends on the nonunique FP that represents the CHM (Weeks 1995).

The tessellating group Γ is generated by a number N (equal to the number of faces in the FP) of basic motions, or generators g_k , $k = 0$ to $N - 1$, in the sense that their products, in any number and order, produce the cells that tessellate H^3 . Not all these products are independent, since there are relations between the generators. See Fagundes (1989), in which one such model is dealt with in some detail. There, as here, I take the density parameter Ω_0 equal to 0.1, which

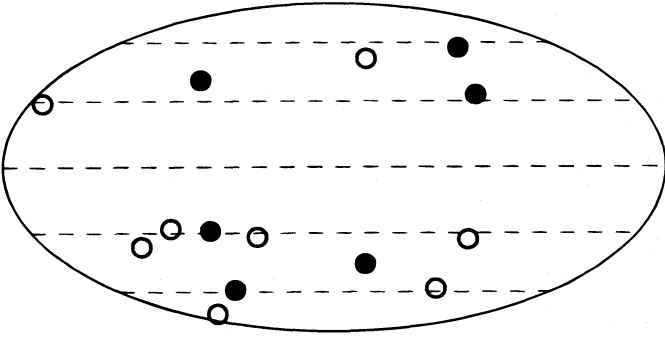


FIG. 1.—Mollweide map of Cayón-Smoot spots. Open circles are underdense (“hot”) spots, and filled circles are overdense (“cold”) spots.

leads to the horizon at $\chi = 3.6369$. To fill the sphere bounded by the surface of last scattering at $Z_{\text{rec}} = 1400$, we need about 2000 cells, each corresponding to an independent product of generators (or independent *word*, in group-theoretical parlance). Each word corresponds to a rigid motion in H^3 , which is defined operationally by a Lorentz transformation matrix (related to the representation of H^3 as the upper sheet of hyperboloid $X^2 + Y^2 + Z^2 - W^2 = -1$ in an abstract Minkowski space). The matrices for the generators are obtained instantly from the excellent software SNAPPEA, developed by Weeks (1992), which one can obtain by anonymous ftp from the University of Minnesota’s Geometry Center.

The first of the CHMs used below is the 18 face Weeks-Matveev-Fomenko manifold. It is described succinctly in Fagundes (1993), and its FP is shown in Figure 24 of Lachièze-Rey & Luminet (1995). In the Appendix, I list the matrices for its even-numbered generators, the odd-numbered ones being the inverses: $g_{2n+1} = g_{2n}^{-1}$, $n = 0-8$.

3. CAYÓN-SMOOT SPOTS AS IMAGES OF SEEDS INSIDE THE FUNDAMENTAL POLYHEDRON

For each of the manifolds in Hodgson & Weeks’s (1994) list of the 10 known orientable CHMs with the smallest volumes (these range from 0.942707 to 1.440699 in the standard normalization of the curvature to $K = -1$), I consider a closed hyperbolic universe model, numbered HW01–HW10. A computer program built a data file for each of them, with the independent words for motions that take the center of the FP into a point inside the region limited by spheres of radii $\chi_{\text{rec}} \pm \text{inradius}$, where $\chi_{\text{rec}} = 3.4768$ corresponds to the (average) recombination time as seen from the center of the FP, and $\text{inradius} \approx 0.5$ is the radius of the sphere inscribed in the FP. (I considered words made up of up to five generators, which fill more than 93% of that region. This can be improved to 100% by adding six-generator-long words, at the cost of much longer computer times.) The margins around χ_{rec} were needed to leave room for Earth’s positions off the center of the FP, as required by Copernicus’ principle. The data files also contain the locations of the centers of the cells (images of the center of FP), which are used in the search for new independent motions: a new word is discarded if it leads to the same center as a previously found independent one.

It is understood that the patches of matter inhomogeneity that left their imprints on the DMR maps were in thermal equilibrium with radiation in the shell $Z_{\text{rec}} \pm \Delta Z$, where $\Delta Z \approx 80$ (White et al. 1994). But since this shell corresponds to an angular scale of a few arcminutes, its effect is

smeared out in the wide angle DMR, together with the other small-scale effects. So, after subtraction of the dipole anisotropy (Doppler shift due to Earth’s motion with respect to the CMB), the map looks like a Planckian distribution at $T = 2.726$ K, except for the tiny, large-scale fluctuations $\Delta T \approx 30 \mu\text{K}$, interpreted as Sachs-Wolfe redshift deviations and thus indicating matter inhomogeneity. Therefore, for this work’s purpose, we can consider the shell $Z_{\text{rec}} \pm \Delta Z$ as a surface of last scattering (SLS) at the mean value Z_{rec} .

A sequence of positions and orientations for Earth’s reference system, with respect to SNAPPEA’s working coordinates, was chosen pseudorandomly (the work was programmed in C language on an Apollo HP 750 workstation) for each of the studied universes. The idea is to find points in the FP with images at Z_{rec} and inside a circle of 7° radius centered on one of the CS spots.

Figure 2 is a schematic chart of this search: the polygons represent the FP and one of its replicas, $g(\text{FP})$, where $g \in \Gamma$. Motion g takes the center C of the FP into gC , the center of $g(\text{FP})$, inside the above mentioned range, $\chi_{\text{rec}} \pm \text{inradius}$. We look for a trial image of O , the observer’s position (this choice is not unique) at gO . This trial image is selected for further processing if its direction falls within 7° of the barycenter of one of the CS spots; keeping this direction fixed, the redshift is adjusted at exactly Z_{rec} to obtain an image at I on the SLS, which implies a source at $S = g^{-1}I$. Finally, this image and source are accepted only if S falls within the

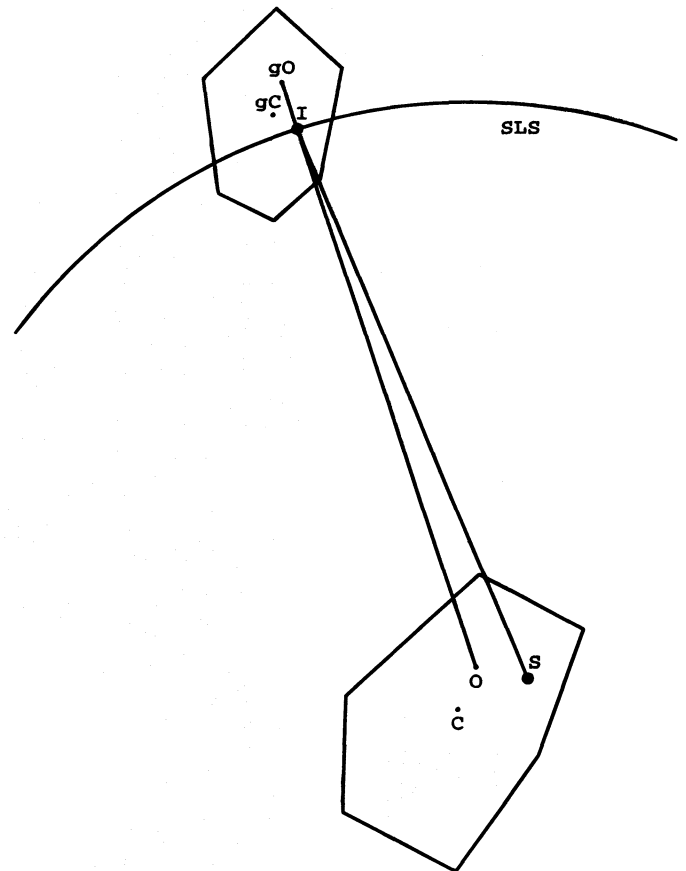


FIG. 2.—Diagram illustrating the search for sources S of spots I . The lower polygon represents the FP; the upper one represents its image under $g \in \Gamma$. C is the center of the FP, O is the observer’s position, and SLS is the surface of last scattering.

TABLE 1

BELTRAMI-KLEIN COORDINATES FOR THE POSITIONS AND EULER ANGLES FOR THE AXES' ORIENTATIONS OF THE OBSERVERS' REFERENCE SYSTEMS, FOR THREE MODELS THAT FIT CAYÓN-SMOOT SPOTS

MODEL	OBSERVER NUMBER	COORDINATES OF ORIGIN			EULER ANGLES ^a		
		<i>x</i>	<i>y</i>	<i>z</i>	ϕ	θ	ψ
HW01.....	682	-0.06446	0.03964	-0.38125	1.19152	0.51634	2.39889
HW05.....	1254	-0.10936	-0.07262	-0.40294	3.55650	0.90578	1.77292
HW07.....	1361	-0.08378	-0.31790	-0.30470	2.37860	2.63253	0.58832

^a In units of radians.

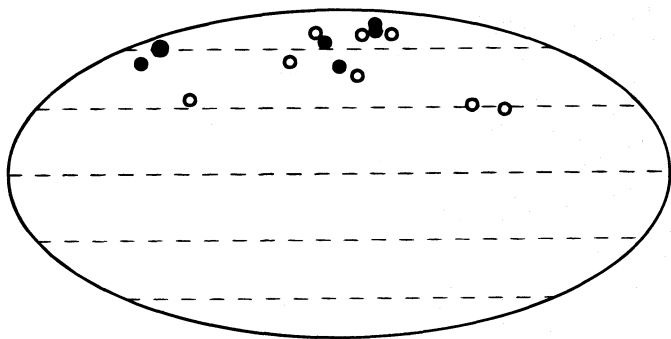


FIG. 3.—Sources for Cayón-Smoot spots, in universe model HW01. Open circles are underdense sources, and filled circles are overdense sources. The larger one would be the seed for the UMa supercluster.

inscribed sphere, with radius χ = inradius; this is to guarantee that S lies inside the FP, but of course it excludes many points from consideration. A future refinement would be to allow as S any point inside the FP. S may also have images in a large number of other cells, $\gamma(\text{FP})$, $\gamma \in \Gamma$, $\gamma \neq g$, perceived at different distances and hence ages (thus facilitating a study of evolution, if and when observations are able to verify the predictions of these models). A few of these extra images might be located inside the shell $Z_{\text{rec}} \pm \Delta Z$ and so produce other spots in the DMR maps; this also will need to be taken into account in an amplified study.

The search for one solution was done by examining up to 2000 observers' reference systems in each of the 10 CHMs in Hodgson & Weeks (1994). The Beltrami-Klein coordinates

TABLE 2

POSITIONS OF CAYÓN-SMOOT COLD SPOTS AND THEIR SOURCES IN THREE UNIVERSE MODELS WITH CLOSED SPATIAL SECTIONS OF NEGATIVE CURVATURE

COLD SPOTS (<i>l</i> , <i>b</i>) ^a	SOURCES								
	Model HW01			Model HW05			Model HW07		
	<i>Z</i>	<i>l</i>	<i>b</i>	<i>Z</i>	<i>l</i>	<i>b</i>	<i>Z</i>	<i>l</i>	<i>b</i>
-99, 57	0.58	145	52	0.42	55	43	0.79	20	-19
85, 40	0.06	151	61 ^b	0.83	5	22	0.96	26	-15
-21, -45	0.76	-1	50	0.73	9	31	0.52	111	-19
73, 29	0.54	-40	71	0.80	12	52	0.69	38	-16
82, -59	0.58	-48	75	0.61	-15	66	0.06	58	55 ^c
-86, 33	0.62	12	64	0.07	50	55 ^c	1.04	58	-37

^a Galactic coordinates *l*, *b* in degrees.

^b Near mean position of UMa supercluster at (*Z*, *l*, *b*) = (0.058, 142, 60).

^c Near mean position of CrB supercluster at (*Z*, *l*, *b*) = (0.071, 48, 56).

TABLE 3

POSITIONS OF CAYÓN-SMOOT HOT SPOTS AND THEIR SOURCES IN THREE UNIVERSE MODELS WITH CLOSED SPATIAL SECTIONS OF NEGATIVE CURVATURE

HOT SPOTS (<i>l</i> , <i>b</i>) ^a	SOURCES								
	Model HW01			Model HW05			Model HW07		
	<i>Z</i>	<i>l</i>	<i>b</i>	<i>Z</i>	<i>l</i>	<i>b</i>	<i>Z</i>	<i>l</i>	<i>b</i>
-24, 51	0.93	-97	29	0.66	9	49	0.66	39	-12
46, -32	1.11	24	70	0.67	-23	7	0.71	37	-21
96, -28	0.52	-55	69	0.65	9	42	0.28	75	-5
120, -37	0.99	-24	68	0.63	3	35	1.02	26	-29
172, 29	0.66	-79	31	0.44	-28	17	0.68	35	-16
-81, -33	0.92	36	53	0.56	22	51	0.64	52	-46
141, -74	0.48	91	34	0.63	12	40	1.35	64	-19
-83, -58	0.93	-12	46	0.94	-59	59	0.38	33	-59

^a Galactic coordinates *l*, *b* in degrees.

(defined in Fagundes 1989 as x_i , $i = 1-3$) of their origins and Euler angles (ϕ , θ , ψ , as in Goldstein 1959, pp. 107–109) of their axes' orientations were chosen pseudorandomly, and I looked for sources of the CS spots as sketched above. A further constraint was that the first seed obtained for a cold spot in the CS list was located near one of three rich superclusters of galaxies: UMa (BS8 in Bahcall & Soneira 1984), CrB (BS12B), and Her (BS15), within $|\delta Z/Z| \leq 0.2$, and (l , b) inside a disk of radius 7° around the supercluster's mean position. Superclusters are only cataloged up to about $Z = 0.08$ (Bahcall & Soneira 1984); these are located inside a ball of radius $\chi = 0.073$, which occupies less than 0.2% of the FP's volume, presumably filled with superclusters. So it would be unreasonable to require more than one of the six cold spots to have as sources the seeds for known superclusters. Similarly, no attempt was made to fit one of the underdense sources to the position of the Boötes void (Kirshner et al. 1981). When superclusters and voids are cataloged up to about $Z = 1$, and many more physical spots are identified on the SLS, then we should try to interpret their sources as original seeds for many superclusters and voids.

For models based on five of the 10 Hodgson & Weeks spaces, the above outlined method produced one solution. I chose three of these, based on HW01, HW05, and HW07, that appear to be the most illustrative. Their Beltrami-Klein coordinates and Euler angles are listed in Table 1. The results are given in Tables 2 and 3, and for universe HW1 a map of the sources is also shown in Figure 3.

4. DISCUSSION

Since the outer radii of our manifolds are $\chi_{\text{out}} \geq 0.75$, and the radius of the SLS sphere is $\chi_{\text{rec}} = 3.4768$, a distant cell subtends an angle $\geq 1.5/\sinh(3.48)$ $rd = 5^\circ.3$, much larger than the $0^\circ.9$ upper limit for causal homogenization; see Weinberg (1972), p. 525. See also Gott (1980). So we may still need something like inflation to account for early homogenization, unless much smaller CHMs are discovered; see Hayward & Twamley (1990) on the latter possibility. Inflation leading to bubble universes of negative spatial curvature has been studied by Gott (1982, 1986) and others; see García-Bellido (1995) and references there. These studies deal with the simply connected FRW open model, but they can probably be adapted to closed hyperbolic universes.

On the other hand, the above lower limit (in our sample of ten manifolds) of $5^\circ.3$ for the angle subtended by a cell may be too small to reconcile with low-order multipoles obtained from the COBE data (I thank the referee for this remark). But that angle can be increased in two ways. First, it increases with the density parameter (since χ_{rec} decreases): for $\Omega_0 = 0.3$, it is $16^\circ.7$, and for $\Omega_0 = 0.5$ it is $32^\circ.2$. Second, we might discard the smallest CHMs and choose one with bigger diameter: the icosahedron manifold used in Fagundes (1989), obtainable from Weeks's (1992) SNAPPEA

program as v3519(2, 1), has outer radius = 1.3826, hence the subtended angle is $9^\circ.8$ for $\Omega_0 = 0.1$ and $30^\circ.9$ for $\Omega_0 = 0.3$.

A nontrivial topology keeps its interest even if the FP is not small; see Ellis & Schreiber (1986) and Fagundes (1992). The cells in the present models have diameters of at least $3283 h^{-1}$ Mpc. So they probably can withstand constraints similar to those obtained by Stevens, Scott, & Silk (1993), Oliveira-Costa & Smoot (1995), and others; besides, Cornish, Spergel, & Starkman (1996) argue that these constraints, obtained from analyses of closed Euclidean models, are completely invalid for closed hyperbolic ones.

In principle, the above results could be interpreted as narrowing the possibilities of closed hyperbolic models and so helping to find the correct topology of the universe. But these are preliminary, tentative calculations, depending on several assumptions and shortcuts. An added complication on the CMB (also a referee's remark) would be the need to take into account fluctuations produced on the original radiation in its way to us, by intervening growing matter fluctuations. As these and other constraints have to be satisfied, such as reducing the positional errors from 7° to 1° or 2° , or a fitting of the seeds of several superclusters and voids, the method will be more selective on the allowed CHMs. On the other hand, there are by now over 11,000 known orientable CHMs (Weeks 1995) in principle usable as spatial sections. And of course we can increase the number of trial random observers in each CHM to, say, a million or more.

In any case, many checks should be necessary to investigate the multiconnectedness. Several ideas have been tried on the distribution of cosmic objects that could be interpreted in terms of multiple images, say, of galaxies and quasars and their clusters; cf. Lachièze-Rey & Luminet 1995, § 11. But the results have been inconclusive, which is understandable given the large distances and time spans involved, the lack of a reliable theory of galactic evolution, and present observational limitations. Two recent proposals look promising: Lehoucq, Lachièze-Rey, & Luminet (1996) suggest looking at the distributions of the distances between images of cosmic sources and comparing them with the predictions from different topologies. Cornish et al. (1996) point out that the spherical SLS "crosses back on itself and self-intersects" along circles; the eventual discovery and study of such circles might help to establish the topology.

Considering present limitations, plus the many uncertainties of cosmological theory, the numerical results of this paper should not be taken literally, but rather as suggesting a line of research based on a very attractive idea about the shape of cosmic space.

I am grateful to J. Weeks for continuing correspondence on CHMs; to T. Villela for help on the CMB literature; and to Conselho Nacional de Desenvolvimento Científico e Tecnológico (CNPq - Brazil) for partial financial support.

APPENDIX

Manifold HW01 is the smallest known CHM, with volume = 0.942707, inradius (radius of inscribed sphere) = 0.519162, and outradius (radius of circumscribed sphere) = 0.752470. It was discovered independently by Weeks (1985) and Matveev & Fomenko (1988).

The matrices for the even-numbered generators g_{2n} , $n = 0-8$, are given below. They were obtained from the 1992 version of Weeks's program SNAPPEA (and here shortened to 10 decimals). For the odd-numbered generators, $g_{2n+1} = g_{2n}^{-1}$.

$$\begin{aligned}
g_{00} &= \begin{pmatrix} 0.9246749551 & 0.9241576804 & 0.1291189968 & -0.8519171944 \\ 0.5193033892 & 1.0731781232 & -1.3739639657 & -1.5195934566 \\ -0.5183538823 & 1.0054161043 & 0.0046049294 & -0.5287470998 \\ -0.6272085219 & -1.4200845909 & 0.9510362242 & 2.0771376158 \end{pmatrix} \\
g_{02} &= \begin{pmatrix} 0.5895108570 & -1.4700738943 & 0.9557453464 & 1.5563063556 \\ -0.2429617945 & 1.1357794527 & 0.5653371464 & -0.8176988981 \\ -0.8441201362 & -0.6591046787 & 0.2771676979 & 0.4730536065 \\ 0.3450975058 & -1.6986851378 & 0.5566661378 & 2.0771376158 \end{pmatrix} \\
g_{04} &= \begin{pmatrix} 0.0625745390 & 0.8752946057 & -0.9346977876 & -0.8023192469 \\ 1.0368841938 & 0.2592993525 & -0.0117978622 & -0.3774972517 \\ 0.4190713452 & -0.4764241078 & -1.1562587460 & -0.8599622147 \\ -0.5046436333 & -0.2456760704 & 1.1003333274 & 1.5892625207 \end{pmatrix} \\
g_{06} &= \begin{pmatrix} -0.7268737654 & -0.4886200786 & 0.4949177714 & 0.1097207929 \\ 0.6732896785 & 0.5930942741 & 1.3026847345 & -1.2255885634 \\ -0.6267699178 & 0.7756992631 & -0.1307650722 & 0.1079322967 \\ -0.6119681297 & -0.4384287238 & -0.9793010886 & 1.5892625207 \end{pmatrix} \\
g_{08} &= \begin{pmatrix} -0.3814233603 & -0.8208918389 & 0.5876832603 & 0.4058556461 \\ -1.4483972995 & 0.3422284579 & 0.3332311230 & 1.1515285649 \\ -0.4398113399 & -0.4574466568 & -0.7951899520 & 0.1871323552 \\ -1.1986544672 & -0.0155297269 & 0.2978953769 & 1.5892625207 \end{pmatrix} \\
g_{10} &= \begin{pmatrix} -0.9660700364 & 0.8213410673 & 0.4654805962 & -0.9080554220 \\ -0.4620725909 & -0.9823131949 & -0.4946255573 & 0.6504650137 \\ -0.0992443281 & -0.1650580379 & 1.1139983768 & -0.5273385783 \\ 0.3957926618 & -0.8165687464 & -0.8380447547 & 1.5892625207 \end{pmatrix} \\
g_{12} &= \begin{pmatrix} 0.6357748696 & 0.2013626321 & -0.9508632837 & -0.5906755274 \\ -0.2197228688 & -0.9265999845 & -0.8076604341 & -0.7477840913 \\ -0.9563175976 & 0.8381185589 & 0.0262805515 & 0.7859241272 \\ -0.6058309759 & 0.7756140533 & 0.7464228216 & 1.5892625207 \end{pmatrix} \\
g_{14} &= \begin{pmatrix} 0.6308944083 & -0.6698401734 & 1.2797572014 & -1.2183973518 \\ 0.4996778790 & -0.7408517185 & -0.4778928577 & -0.1640756990 \\ 0.7619863709 & 0.6401733903 & -0.1545872533 & 0.1197598341 \\ 0.4778378036 & 0.6382547268 & -0.9434284800 & 1.5892625207 \end{pmatrix} \\
g_{16} &= \begin{pmatrix} 0.1481741386 & -0.9356287990 & 0.4235925724 & -0.2771055615 \\ 1.2068325480 & 0.1359125410 & -0.8253394744 & 1.0752219612 \\ -0.1471289931 & 0.3273590617 & 1.7183713280 & -1.4427788870 \\ 0.7071402371 & -0.0322090600 & -1.6773240404 & 2.0771376158 \end{pmatrix}
\end{aligned}$$

In the data file of motions that take the center of the FP into the region between radii $\chi_{\text{rec}} \pm \text{inradius}$, the first word is $g_{00} g_{00} g_{00}$ and the last one is $g_{14} g_{01} g_{10} g_{05} g_{08}$.

REFERENCES

- Bahcall, N. A., & Soneira, R. M. 1984, *ApJ*, 277, 27
 Bennett, C. L., et al. 1994, *ApJ*, 436, 423
 Cayón, L., & Smoot, G. 1995, *ApJ*, 452, 494 (CS)
 Cornish, N. J., Spergel, D. N., & Starkman, G. D. 1996, preprint gr-qc/9602039
 Ellis, G. F. R., & Schreiber, G. 1986, *Phys. Lett.*, A115, 97
 Fagundes, H. V. 1989, *ApJ*, 338, 618; erratum, 349, 678 (1990)
 ———. 1992, *Gen. Relativ. Gravitation*, 24, 199
 ———. 1993, *Phys. Rev. Lett.*, 70, 1579
 ———. 1995, preprint IFT-P-010/95
 García-Bellido, J. 1995, preprint astro-ph/9511078
 Goldstein, H. 1959, *Classical Mechanics* (Reading: Addison-Wesley)
 Gott, J. R. III. 1980, *MNRAS*, 193, 153
 Gott, J. R. III. 1982, *Nature*, 295, 304
 ———. 1986, in *Inner Space/Outer Space*, ed. E. W. Kolb et al. (Chicago: Univ. Chicago Press), 362
 Hayward, G., & Twamley, J. 1990, *Phys. Lett.*, A149, 84
 Hodgson, C. D., & Weeks, J. R. 1994, *Exp. Math.*, 3, 261
 Kirshner, R. P., Oemler, A., Jr., Schechter, P. L., & Sackett, S. A. 1981, *ApJ*, 248, L57
 Lachièze-Rey, M., & Luminet, J.-P. 1995, *Phys. Rep.*, 254, 135
 Landau, L., & Lifshitz, E. M. 1975, *The Classical Theory of Fields* (Oxford: Pergamon)
 Lehoucq, R., Lachièze-Rey, M., & Luminet, J.-P. 1996, *A&A*, in press
 Matveev, S. V., & Fomenko, A. T. 1988, *Russian Math. Surveys*, 43, 3
 Oliveira-Costa, A., & Smoot, G. F. 1995, *ApJ*, 448, 477

- Smoot, G. F., et al. 1992, ApJ, 396, L1
Stevens, D., Scott, D., & Silk, J. 1993, Phys. Rev. Lett., 71, 20
Torres, S. 1994, preprint ICRA-20-01-94
Weeks, J. R. 1985, Ph.D. thesis, Princeton Univ.
———. 1992, SnapPea, a Computer Program for Creating and Studying
3-Manifolds (available by anonymous ftp from geom.umn.edu)
- Weeks, J. R. 1995, private communication
Weinberg, W. 1972, Gravitation and Cosmology: Principles and Applica-
tions of the General Theory of Relativity (New York: Wiley)
White, M., Scott, D., & Silk, J. 1994, ARA&A, 32, 319
Wright, E. L., Smoot, G. F., Bennett, C. L., & Lubin, P. M. 1994, ApJ, 436,
443